APPLYING PR CONTROLLER TO IMPROVE THE ISLANDING DETECTION TIME OF THE DISTRIBUTION GENERATION

[1]SHENG-KUAN WANG, [2]JIAN-ZHI CHEN

[1,2]Electrical EngineeringDepartment,Ming Chi University of Technology
E-mail: [1]skwang@mail.mcut.edu.tw, jeff20060502@yahoo.com.tw

Abstract - Abstract: A Distribution generation (DG) test system includes a software phase-locked loop, a power controller and islanding detection technology, which is implemented in this paper. Two types of power controllers, proportional-integral (PI) and proportional-resonant (PR), are compared in terms of the transient response. The PI controller is only used when there is a DC signal. The abc frame uses a Park transformation to the synchronized reference frame to produce the DC signals, which requires much calculation time, but the DC control signal is more stable than AC. The PR controller can operate in the AC mode, which saves the time that is taken for the transformation. The PR controller includes a two-order filter, but the output signal is slightly more unstable than that for a PI. The islanding detection time is affected by the transient response of the power controller. An islanding detection method that uses the rate of change of frequency is used in the DG test system. The experimental results show that the PR controller has a faster transient response and that it detects islanding events faster than a PI controller.

Keywords - Proportion-integral controller, Proportion-resonance controller, Distribution generation, Anti-islanding operation.

I. INTRODUCTION

A renewable energy source is usually classified as a distributed generation (DG) because its capacity is usually small and it is installed near the load. In recent years, distributed energy resources have garnered more attention because they are more environmentally friendly. Traditional centralized power plants are far from the load center, so the electrical power is delivered along transmission lines, which results in power loss. Many distributed energy resources, such as solar and wind energy, are intermittent. The stability of the power supply is an important factor in the design of a DG system. Therefore, most DGs are connected to the grid to increase the reliability of the power supply. The output terminal of an inverter-based DG is connected to a low-pass filter to eliminate high-frequency harmonics. The output voltage of the inverter is controlled by a sine pulse width modulation (SPWM) module. A software phase-locked loop (SPLL) is used to measure the magnitude, the phase and the frequency of the grid voltage in the DG in order to synchronize the output voltage of the DG.

A Proportional-Integral (PI) controller is often in a SPLL and in power control units for a DG [1], but a PI controller only operates in DC. Therefore, the voltage signals in a three-phase abc frame must be transformed to the dq frame of the synchronized reference frame using a Park transformation [2], which increases the time that is taken for the transient response of the controller. In recent years, Proportional-Resonant (PR) controllers have been used in controllers to reduce the time that is taken for the transient response. A PR controller is only used in the AC mode, so there is no need for a Park transformation [3]. A three-phase abc frame must be transformed to the αβ frame of the stationary reference frame using a constant matrix if a PR-based power controller is used. A PR controller can also be designed to eliminate the specific harmonic frequencies [4]. In the DG test system, the SPLL is a PI controller but the power controller uses a PR controller, in order to allow fast detection of islanding operation. The two-order filter in a PR controller eliminates almost harmonic frequencies, except the 60Hz element, which has a smaller steady-state error. The transfer function for a PR controller must be discretized, in order to allow it to be implemented on a digital signal processor (DSP) [6].

In a single-phase DG system, AC signals cannot be directly transformed to the dq frame using a Park transformation when a PI-based controller is used because a Park transformation is only relevant to a three-phase system. A single-phase DG system must also be connected to the grid, so a SPLL must be used. A Second-Order Generalized Integrator (SOGI) is widely used to address this problem [7]. A SOGI produces a sine wave signal that lags the fundamental voltage by 90 degree, so the single-phase frame becomes the αβ frame. A single-phase system can also be transformed to the dq frame using a Park transformation so the power controller for a three-phase system has fewer adjustable parameters. In a three-phase system, the general control paths for active and reactive power require individual PR controllers, which have four adjustable control parameters. If the PR power controller only inputs the phase-a signal to produce the correction value, which is expanded to the αβ frame by the SOGI, this power control method is faster because it only requires the adjustment of two PR parameters. The transform function for a SOGI is similar to that for a PR, so it is easily implemented. This study determines the

feasibility of using a PR and SOGI to control the power.

When the DG is connected to the grid, islanding operation must be avoided to ensure the operation of the DG. During islanding, the DG is disconnected from the grid, but the DG does not perceive a continuous supply of power to the local load. Islanding operation can cause electric shocks to maintenance workers. The output voltage and the output frequency of the DG are unstable when the DG is disconnected from the grid, which reduces the lifetime of the electrical equipment. The magnitude, phase and frequency of the voltage in a DG are asynchronous with the grid. When the grid is suddenly reconnected to the DG, a large fault current can occur in the DG. This study uses the Rate of Change of Frequency (ROCOF) to prevent islanding in the DG. The ROCOF method uses the variation in the frequency to detect islanding events. The circuit breaker at the DG side is tripped to protect the DG when an islanding event occurs. This study uses a PR power controller to decrease the time that is required to detect islanding events.

II. STRUCTURE OF THE TEST SYSTEM

The DG system is connected to the grid as shown in Fig.1. The output stage for the DG is an inverter. The inverter is connected to the LCL filter [8], the isolation transformer and the local load for the grid. The isolation transformer uses delta-connection to eliminate the third-order harmonic at the grid terminal and to isolate any interference due to the common-mode signal between the DG and the grid. The location of the load is called the Point of Common Coupling (PCC) in Fig. 1. Circuit breakers SW2 and SW1 are closed when the DG is connected to the grid. Circuit breaker SW2 simulates the scenario whereby the DG is disconnected from the grid, so the output power from the DG supplies all of the power to the local load. Circuit breaker SW1 is tripped when the DG is subject to an islanding event. If the output power from the DG and the demand from the load are unbalanced before SW2 is tripped, then the physical values for the frequency, the magnitude and the phase of the voltage and current, the harmonics and the load power at the PCC oscillate from one steady-state operation to another. Passive islanding detection uses the change in the physical value to distinguish an islanding event. Islanding detection using the ROCOF method detects the rate of change of the frequency of the supply at the PCC to identify an islanding event.

The grid is considered to be an infinite bus when the DG is connected to the grid. The magnitude of the output voltage for the DG is maintained at the grid voltage. Variations in the internal voltage of the DG affect the magnitude and phase of the output current from the DG, which are controlled by the SPWM module. Therefore,the output power of the DG is controlled by the feedback from the inverter output current to theinput terminal of the power controller.

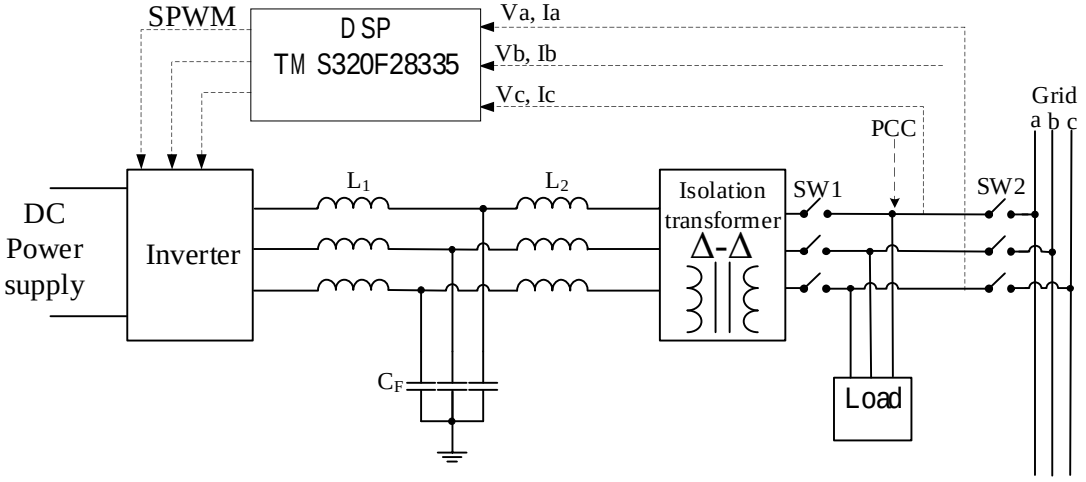


Fig. 1 The test system for a DG connected to a grid

This feedback circuit controls the power. Initially, a LA55-P Hall current sensor is used for the current feedback circuit, as shown in Fig. 2. However, this circuit does not allow easy correction of the level and span. An ACS712 current sensor module is used in Fig. 3. The maximum input current for the ACS712 is 20A and the output voltage ranges from 0 to 5V, so it is suitable for the 3kW DG test system. Output currents of 0−3kW from the DG are measured by the ACS712, which outputs a voltage from 1.5 to 3.5V. The voltage must be reduced to 1.0V so that the limit for the DSP input voltage is not exceeded, as shown in Fig. 3. The disadvantage of the ACS712 is that it cannot be used when the current approaches zero because the module cannot accurately measure the real current.

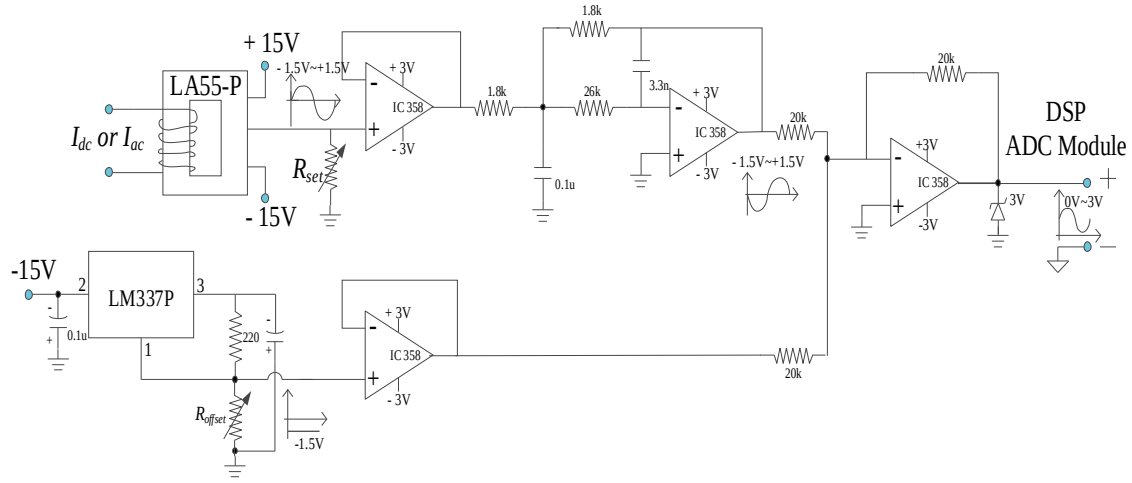


Fig. 2 The current measurement circuit for a LA55-P current sensor

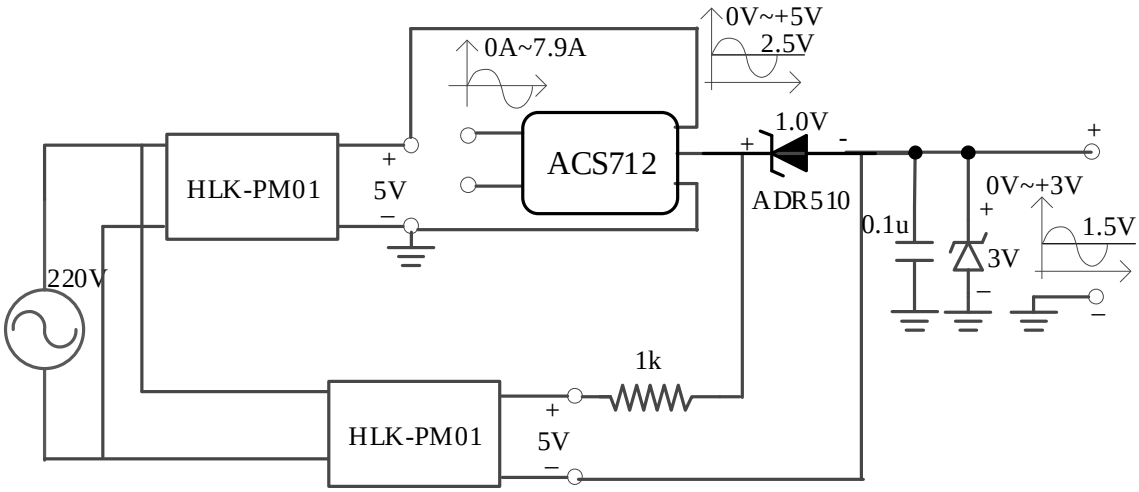


Fig. 3 The current measurement circuit for an ACS712 current sensor

III. THE CONTROLLERS IN THE DG

The synchronized reference frame (SRF) is used for SPLL in this study, which is shown in Fig. 4. The three-phase abc frame is transformed to the dq frame using a Park transformation. The difference in the phase-angles, $\Delta\theta$, between v_a and V_d is calculated as V_q/V_d. If the PI controller makes a phase angle of v_a and V_d to tends zero, then the value of V_q approaches zero and the value of V_d is equal to v_a. The current angular speed of the PCC is calculated as the sum of the rated angular speed and the output from the PI controller. The phase angle a is calculated as the integral of the final angular speed. If the value of V_d isnegative, the output phase angle for the SPLL must be 180 degree out of phase to obtain the correct angle.

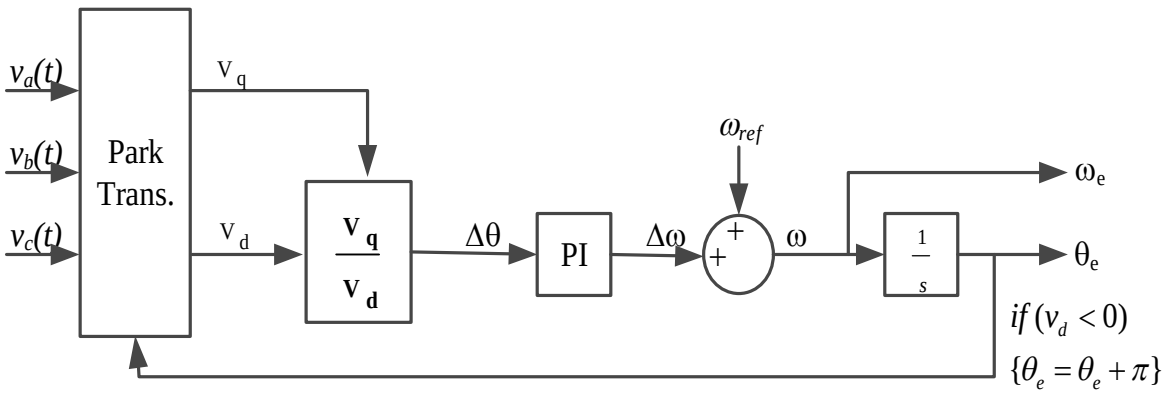


Fig.4 SRF-SPLL

The power controller for the DG is a PI-based controller, as shown in Fig. 5. The settings for the active and reactive power in Fig. 5 are transformed to the settings for the currents I_{d_set} and I_{q_set}. The output current from the DG in the abc frame is fed back as $I_d$and I_q. The errors between the set and the feedback currents in Fig. 5 are Δi_d and Δi_q. The error is reduced to zero by the PI controllers. The output signals from the PI controllers are $\Delta V_d$and ΔV_q, which are added to V_d and V_q for the SPLLoutput signals to calculate the input voltage signal for SPWM. All of the control signals in the power controller are DC, which gives greater stability. The correct DC signals in the power controller must experience an integral period of rated system frequency. Therefore, DC signals cannot instantly respond to a variation in the AC current.

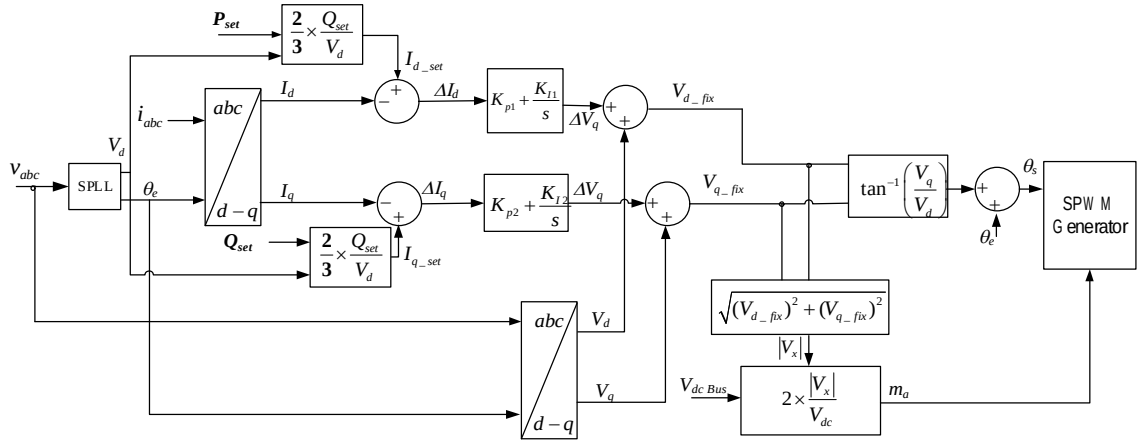


Fig. 5 A PI-based power controller

PR controllers have replaced PI controllers in power control loops, as shown in Fig. 6. A PR controller differs from a PI controller in that it uses AC control signals, rather than DC. The abc frame is transformed to the αβ frame using a Clarke transformation, but the transformation matrix is constant so it requires less calculation time than a Park transformation. Therefore, the computational burden for the DSP is reduced and the settings for the AC current can be easily tracked. This study uses two PR controllers for fast detection of islanding events.

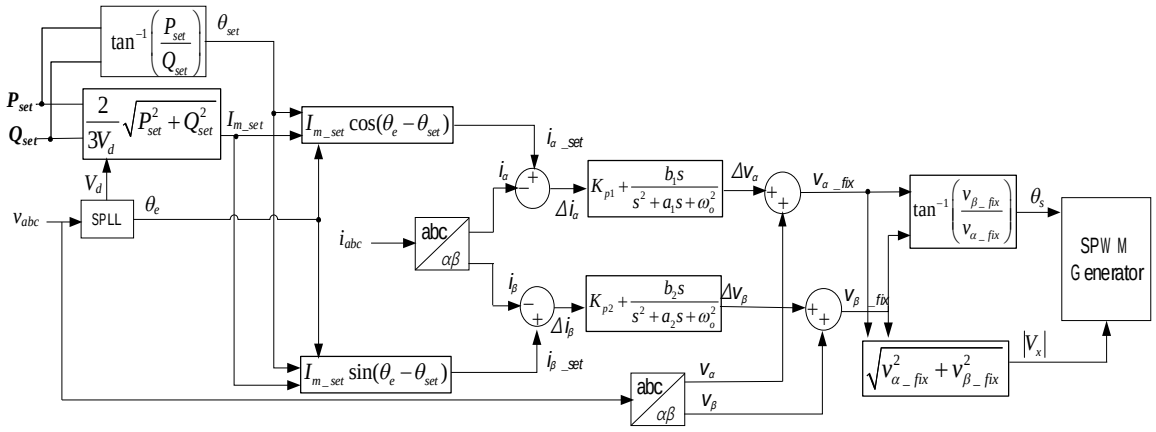


Fig. 6 The power controller for two PR controllers

The transform function for a PR controller (1) is discretized by z-transformation, in order to allow it to be implemented with the DSP [10]. Y and U are the output and input variables. The second term in (1) is transformed from the s-domain to the z-domain using (2) and the result is (3). The coefficients for the standard formulation of second order in (4) are obtained after comparison with (3), as shown in (5). Equation (6) is derived using the cross multiplication and shift term from (4), where z^{-1} and z^{-2} respectively represent the state values of the last time and the time previous to last. Equation (6) is rewritten in the form of the time-domain as (7), in which Y and U in the z-domain are replaced by y and u and the terms z^{-1} and z^{-2} are represented as y(t-1) and y(t-2).

$$H(s) = K_p + \frac{bs}{s^2 + as + \omega_o^2} \tag{1}$$

$$s = \frac{2}{T_s}\frac{1-z^{-1}}{1+z^{-1}} = K_t\frac{1-z^{-1}}{1+z^{-1}};\ \text{where}\ \frac{2}{T_s} = K_t \tag{2}$$

$$\frac{bs}{s^2 + as + \omega_o^2} = \frac{bK_t\dfrac{1-z^{-1}}{1+z^{-1}}}{K_t^{\,2}\left(\dfrac{1-z^{-1}}{1+z^{-1}}\right)^2 + aK_t\dfrac{1-z^{-1}}{1+z^{-1}} + \omega_o^2}$$

$$= \frac{b \times K_t(1-z^{-2})}{K_t^{\,2}(1-z^{-1})^2 + aK_t(1-z^{-2}) + \omega_o^2(1+z^{-1})^2}$$

$$= \frac{bK_t - bK_t z^{-2}}{K_t^2 + aK_t + \omega_o^2 - 2K_t^2 z^{-1} + 2\omega_o^2 z^{-1} + K_t^2 z^{-2} - aK_t z^{-2} + \omega_o^2 z^{-2}}$$

$$= \frac{\frac{bK_t}{K_t^2 + aK_t + \omega_o^2} + \frac{-bK_t z^{-2}}{K_t^2 + aK_t + \omega_o^2}}{1 + \frac{(-2K_t^2 + 2\omega_o^2)}{K_t^2 + aK_t + \omega_o^2} z^{-1} + \frac{(K_t^2 - aK_t + \omega_o^2)}{K_t^2 + aK_t + \omega_o^2} z^{-2}} \quad (3)$$

$$\frac{Y(z)}{U(z)} = \frac{b_0 + b_1 z^{-1} + b_2 z^{-2}}{1 + a_1 z^{-1} + a_2 z^{-2}} \quad (4)$$

$$\begin{cases} b_0 = \frac{bK_t}{K_t^2 + aK_t + \omega_o^2}, \quad a_1 = \frac{-2K_t^2 + 2\omega_o^2}{K_t^2 + aK_t + \omega_o^2} \\ b_1 = 0 \\ b_2 = \frac{-bK_t}{K_t^2 + aK_t + \omega_o^2}, \quad a_2 = \frac{K_t^2 - aK_t + \omega_o^2}{K_t^2 + aK_t + \omega_o^2} \end{cases} \quad (5)$$

$$Y(z) = b_0 U(z) + b_1 U(z) z^{-1} + b_2 U(z) z^{-2} - a_1 Y(z) z^{-1} - a_2 Y(z) z^{-2} \quad (6)$$

$$y(k) = b_0 u(t) + b_1 u(t-1) + b_2 u(t-2) - a_1 y(t-1) - a_2 y(t-2) \quad (7)$$

This study uses two PR controllers as the power controller for the α and β frame in Fig. 6. The amplitude of the output current from the inverter is$I_{m_set}$and its phase angle θ_{set} is calculated using the values for the settings for active and reactive power, which determines the setting current for the αβ frame i_{α_set} andi_{β_set}. The output current from the inverter in the abc frame is fed back as $I_\alpha$and I_β. The errors between the setting and feedback currents are Δi_α andΔi_β, as shown in Fig. 6. The error signals are reduced by the PR controllers. The output signals from two PR controllers are the Δv_α andΔv_β, which are added to v_α and v_β of the SPLLoutput signals to obtain the input voltage signal for SPWM.

Bode diagram for the PR controller is shown in Fig. 7. This is sued to design theparameters for the controller. The maximum gain occurs at the resonance frequency ω_0 and the gain decays rapidly either side of this resonance frequency. The PR controllers eliminate harmonics. If parameter "a" in (1) is zero, then the output from the PR controller only contains the signal for the resonance frequency. This creates a barrier in the actual circuit, because the system frequency is not fixed at ω_0. The parameter "a" must be reduced to allow stable operation of the DG.

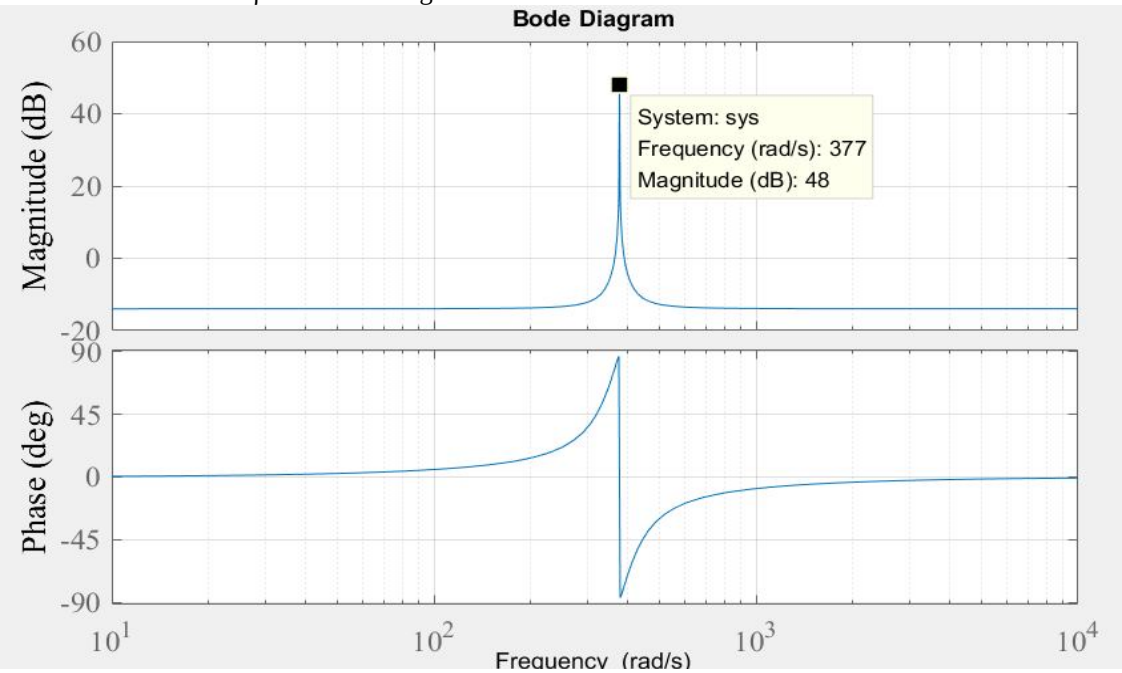


Fig.7 Bode diagram for the PR controller

Another PR-based power controller is shown in Fig. 8. This controller directly uses the current of the phase a as the input signal for the PR controller. The SOGI ensures that the output signal from the PR controller becomes two sine waves of the same magnitude and orthogonal, $v_{\alpha_fix}$and v_{β_fix}. The transform function for the SOGI is shown as (8). The output signals from the SOGI areused to calculatethe magnitude and the phase of the output voltage. The combined PR and SOGI now only require a PR controller, which eliminate two adjustable parameters, and the feedback current in the abc frame need not be transformed to the αβ frame, which decreases the time that is taken fore calculation. The power controller for the combined PR and SOGI in Fig. 8 is better than the two PR controllers that are used in Fig. 6.

$$\begin{cases} H_\alpha(s) = \frac{k\omega_o s}{s^2 + k\omega_o s + \omega_o^2} \\ H_\beta(s) = \frac{k\omega_o^2}{s^2 + k\omega_o s + \omega_o^2} \end{cases} \quad (8)$$

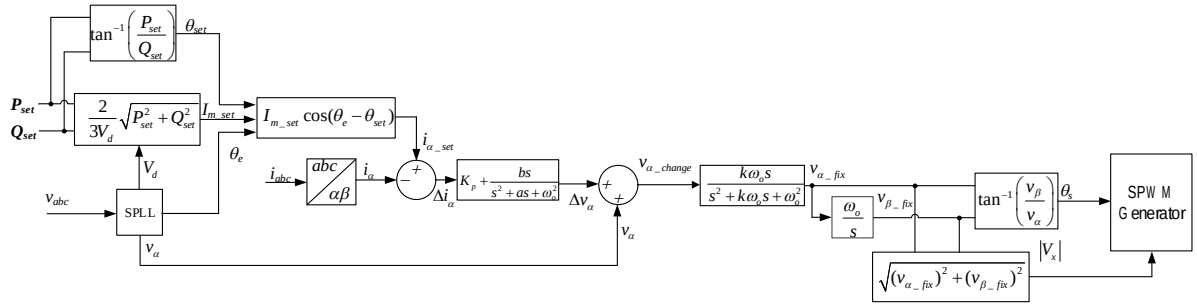
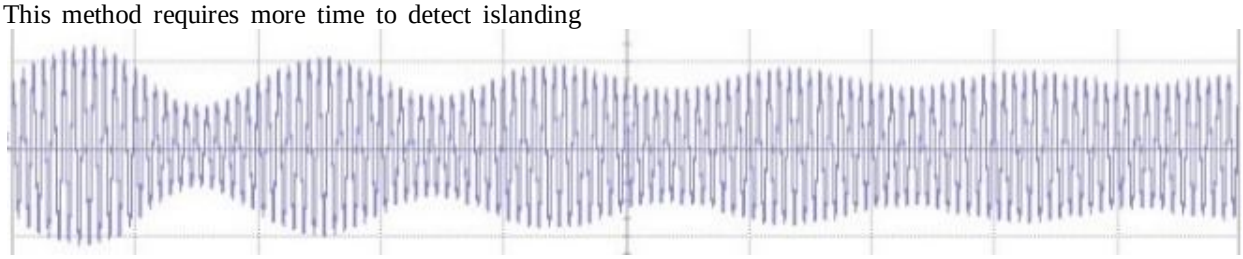


Fig.8 The power controller for a combined PR and SOGI

IV. EXPERIMENTAL RESULTS

The test system in Fig. 1 was implemented with DSP28335 to test the performance of the two type of PR-based power controllers in Fig. 6 and Fig. 8. The output current from the inverter for the combined PR and SOGI method for 0 to 2kW is shown in Fig. 9. The output current from the inverter gradually stabilizes, but the oscillation time is more than 2 sec. This method requires more time to detect islanding than is required for IEEE 1547. The time that is required between the outputs of orthogonal signals from the SOGI to the arctangent function is too long so the power controller cannot track the setting values for the current. The power controller for the combined PR and SOGI has only two adjustable parameters, but its transient response is too slow. Therefore, the power controller for the combined PR and SOGI is not suited to the detection of islanding.



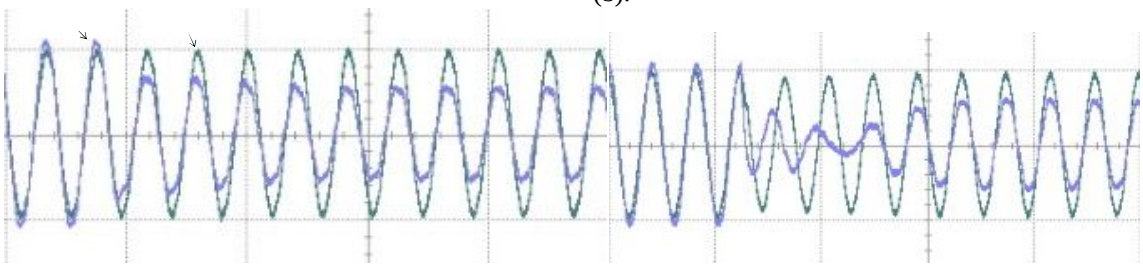
Current:10A/Div Time: 200ms/Div

Fig.9 The output current from the DG for a combined PR and SOGI method

The power controller in Fig. 6 was used for the experiments for variation in power. The transient-response time for the output current is important because it affects the time that is required for islanding detection. The various load conditions include different resistive, inductive and capacitive loads, and a change from inductive to capacitive load, which is sequentially tested. The experimental results are shown in Fig. 10-13, where C1 and C2 represent the output voltage and current from the DG.

4.1 The resistive load

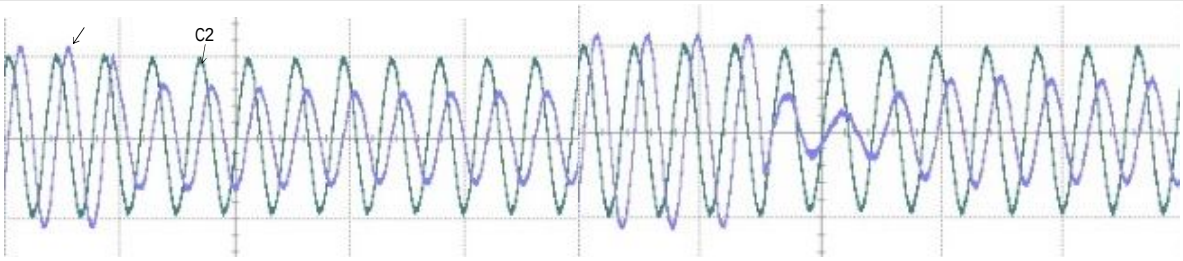
The output power from the DG varies from 3kW to 1.5kW when it is connected to the grid. The oscilloscope readings for the grid voltage and the output current from the DG on the oscilloscope are shown in Fig 10. The transient response for the current is about 3 periods for the PR-based power controller in Fig. 10 (a). This is a better result for the transient-response time than the five periods that are required for the PI-based power controller in Fig. 10 (b).



C1:Voltage 200V/Div C2:Current 10A/Div Time: 40ms/Div
(a) PR controller (b) PI controller
Fig. 10 The output power from the DG from 3kW to 1.5kW

4.2 The inductive load

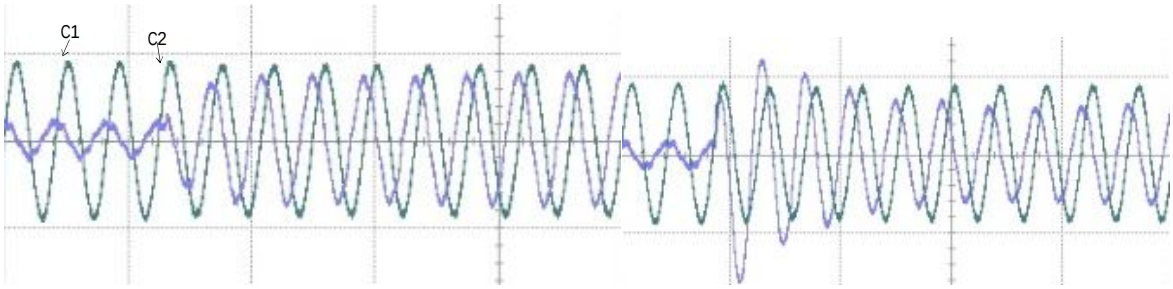
The output power from the DG was varied from +3kVar to +1.5kVar while it was connected to the grid. The oscilloscope readings for the grid voltage and the output current from the DG are shown in Fig 11. The transient response for the current is about 3 periods for the PR-based power controller in Fig. 11 (a). This is a better result for the transient-response time than the five periods that are required for the PI-based power controller in Fig. 11 (b).



(a)PR controller (b) PI controller
C1:Voltage 200V/Div C2:Current 10A/Div Time: 40ms/Div
Fig. 11 The output power form the DG from +3kVar to +1.5kVar

4.3 The capacitive load

The output power from the DG was varied from −500Var to −2kVar while it was connected to the grid. The oscilloscope readings for the grid voltage and the output current from the DG are shown in Fig 12. The transient response for the current is about 2 periods for the PR-based power controller in Fig. 12 (a). This is a better result for the transient-response time than the five periods that are required for the PI-based power controller in Fig. 12 (b).

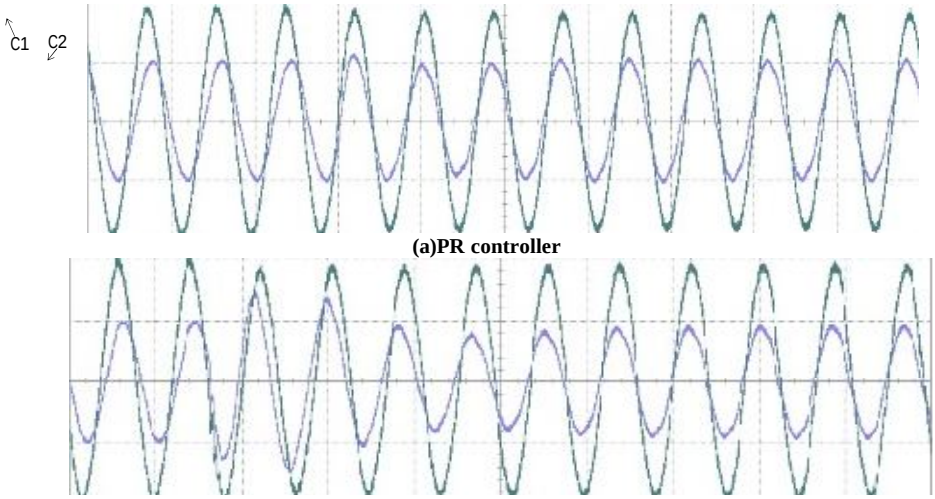


(a)PR controller (b) PI controller
C1:Voltage 200V/Div C2:Current 10A/Div Time: 40ms/Div
Fig .12 The output power from the DG from −500Var to −2kVar

4.4 Change from an inductive to a capacitive load

The output power from the DG was varied from 2.5kW–j1.0Var to 2.5kW+1.0kVar while it was connected to the grid. The oscilloscope reading for the grid voltage and the output current from the DG are shown in Fig 13. The transient response for the current is about 3 periods for the PR-based power controller in Fig. 13 (a). This is a better result for the transient-response time than the eight periods that are required for the PI-based power controller in Fig. 13 (b).

The ROCOF islanding detection method is used in the DG test system for anti-islanding operation. The ROCOF uses the rate of change of frequency at the PCC to detect an islanding event. If the DG supply power and the load demand are unbalanced when the DG is connected to the grid, the grid absorbs or supplies electrical power to the local load.



(a)PR controller

(b) PI controller
C1:Voltage 200V/Div C2:Current 10A/Div Time: 20ms/Div
Fig. 13 The variation of output reactive power of DG from +1kVar to −1kVar

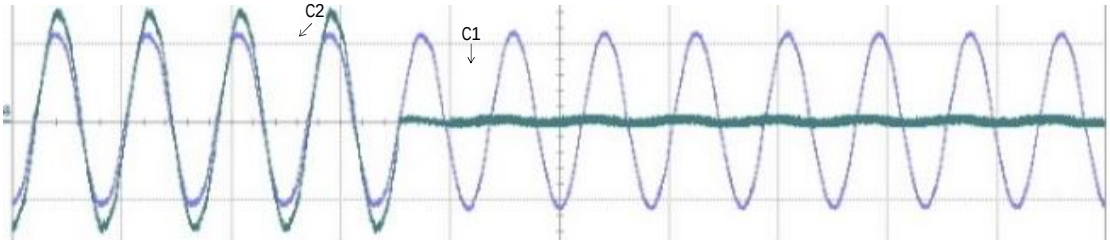
The DG output power cannot be changedinstantaneously when the grid is disconnected fromthe DG, which supplies all of the power to the local load. Therefore, there is a change in the difference in the phase angle between the DG outputcurrent and voltage and the magnitude of the voltage magnitude, so the PCC frequency changes. If the DG output power is equal to the load demand, the PCC frequency does not change when the grid is disconnected so it is difficult to detect islanding. If the rate of change of frequency is detected to be greater than the preset threshold four consecutive times, breaker SW1 in Fig. 1 is tripped to protect the load and the DG. The rate of change of frequency is calculated for each period of the system frequency.

The local load was initially set to the resonance condition of 3kW and a quality factor of 1.0 for IEEE 1547 was used.The output power from the DG was maintained at 3kW using the PR power controller. In this case, the output power from the DG and the load demand are balanced so the grid does not supply power to the local load. The magnitude, phase and frequency of PCC voltage do not change when the grid is disconnected from the DG. The capacitive load was increased in steps of 1% of the rated reactive power to 10%. The threshold for the ROCOF was set to 1.2Hz/s to decrease the frequency of abnormal operation. The experimental results for anti-islanding operation are shown in Table 1.

Table. 1 The islanding detection periods for the ROCOF method for various RLC loads

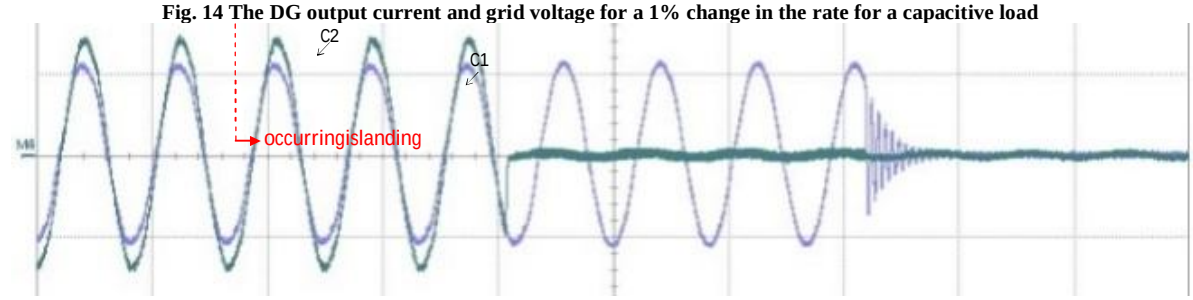
Changing rate of capacitive load	Tripping Periods	Changing rate of capacitive load	Tripping Periods
0	N/A	6%	4
1%	N/A	7%	4
2%	5	8%	3.5
3%	4.5	9%	3.5
4%	4.25	10%	3.5
5%	4.1		

Table 1 shows that the NDZ for the ROCOF is between the 0% and 1%, where 0% signifies that the load operates at the resonance condition, so the DG output voltage and current are in phase. The waves for the grid voltage (C1) and the DG output current (C2) for a 1% change in the rate for a capacitive load are shown in Fig.14, wherein the output current from the DG continuously supplies the load and the grid voltage drops to zero when the test system experiences an islanding event. The PCC frequency varies more during islanding operation when the rate of change in the capacitive load is gradual. Therefore, the detection time for the ROCOF method is faster, as shown in Table 1. The time that is required to detect islanding gradually decreases from 5 to 3.5 periods when the rate of change in the capacitive load is increased from 2% to 10%. The output current from the DG is blocked after about 3.5 periods when there is an 8% change in the rate for the capacitive load after the grid is disconnected from the DG, as shown in Fig. 15.



C1: Voltage 200V/Div C2:Current 10A/Div Time: 20ms/Div

Fig. 14 The DG output current and grid voltage for a 1% change in the rate for a capacitive load



C1: Voltage 200V/Div C2:Current 10A/Div Time: 20ms/Div

Fig. 15 The DG output current and grid voltage for an 8% change in the rate for a capacitive load

CONCLUSION

This paper uses a PR-based power controller in aDG test system to rapidly detect islanding operation. The transient-response time for the power controller affects the time that is required to detect islanding. Two different PR-based power controllers are compared in this study. The experimental results show that the PR power controller for the αβ frame has a faster transient response time than the combined PR and SOGI power controller. The PR-based power controller is used in the DG to test the islanding detection time for the ROCOF method. A 3kW DG test system is used to test the anti-islanding operation.

The experimental results for islanding operation under various capacitive loads show that the tripping time for breaker SW1 is less than 5 periods if the rate of change of the capacitive load is not 0% or 1%, which is the NDZ for the ROCOF.

REFERENCES

[1] Xudong Cao, Hongfeng Zhen, Lingzhi Cui, and Feng Kong,"Active Power Filter Based on DSP digital PI control," International Conference on Future Computer and Communication, Vol. 1, pp. 343-346, May 2010.

[2] Furqan Shaikh, and Binsy Joseph,"Simulation of synchronous reference frame PLL for grid synchronization using Simulink," International Conference on Advances in Computing, Communication and Control, December 2017.

[3] R. Teodorescu, F. Blaabjerg, M. Liserre, and P.C. Loh, "Proportional-resonant controllers and filters for grid-connected voltage-source converters," IEE Proceedings - Electric Power Applications, Vol. 153, No. 5, pp. 750-762, September 2006.

[4] D. Sera, T. Kerekes, M. Lungeanu, P. Nakhost, R. Teodorescu, G. K. Andersen, and M. Liserre,"Low-Cost Digital Implementation of Proportional-Resonant Current Controllers for PV Inverter Applications Using Delta Operator," Annual Conference of IEEE Industrial Electronics Society, pp. 2517-2522, November 2005.

[5] Daniel Nahum Zmood, Donald Grahame Holmes, and Gerwich H. Bode, "Frequency-Domain Analysis of Three-Phase Linear Current Regulators," Conference Record of the 1999 IEEE Industry Applications Conference, Vol. 2, pp. 818-825, October 1999.

[6] Michael John Newman, and Donald Grahame Holmes, "Delta Operator Digital Filters for High Performance Inverter Applications," IEEE transactions on power electronics, Vol. 18, No. 1, pp. 447-454, January 2003.

[7] Mihai Ciobotaru, Remus Teodorescu, and Frede Blaabjerg, "A new single-phase PLL structure based on second order generalized integrator," IEEE Power Electronics Specialists Conference, pp. 1-6, June 2006.

[8] Utsav P. Yagnik, and Mehul D. Solanki, "Comparison of L, LC & LCL filter for grid connected converter," International Conference on Trends in Electronics and Informatics, pp. 455-458, May 2017.

[9] Fei Liu, Xiaoming Zha, Yan Zhou, and Shanxu Duan, "Design and research on parameter of LCL filter in three-phase grid-connected inverter,"International Power Electronics and Motion Control Conference, pp. 2174-2177, May 2009.

[10] Zhou Yan, Duan Shanxu, Liu Fei, and Yin Jinjun, "Research on digital implementation of proportional-resonant controller based on a three-phase PV grid-connected system," International Conference on Electrical Machines and Systems, pp. 2746-2749, October 2008.

[11] Chia-Cheng Lien and Sheng-Kuan Wang "Implementation the rate of change of frequency in the reactive power variation for islanding detection technology," 12th Taiwan Power Electronics Conference & Exhibition, pp. 1-6, Nov. 2, 2013.

[12] Chao-Nan Liu, "Design and Control of a Power Dispatchable Grid-Tied Energy Storage System," Master Thesis, Chang Gung university, July 2016.

[13] Shang-hung Hu, "Design of Resonant Current Controller in Full Stationary-frame for LCL-based Active Front-end Converter," Master Thesis, National Sun Yat-sen university, July 2010.

[14] Raul E. Alzate, and Johnny Posada, "Design and Implementation of Proportional-Resonant Controller for 3-Phase Current Source Inverter in Dspace DS1104," IEEE Workshop on Power Electronics and Power Quality Applications, pp. 1-6, June 2017.

[15] T. M. Rowan, and R. J. Kerkman, "A new synchronous current regulator and an analysis of current regulated PWM inverters," IEEE Transactions on Industry Applications, Vol.22, No.4, pp. 678–690, July 1986.

[16] Tohid Soleimani Aghdam and Hossein Kazemi Karegar, "Settings of ROCOF Relays for Islanding Detection of Wind Turbine, "International Conference on Advanced Power System Automation and Protection, Vol. 2, pp. 1402-1405, October 2011.

★★★